

# OPTIMIZING PROCESS PARAMETERS FOR ENHANCING MECHANICAL PROPERTIES OF AA6061 COMPOSITES REINFORCED WITH WALNUT SHELL ASH AND SILICON CARBIDE

UDC:669.715

Original scientific paper

<https://doi.org/10.46793/aeletters.2024.9.4.5>**Rajesh Angirekula<sup>1</sup>**, **S. Manickam<sup>2</sup>**, **P. Ravindra Babu<sup>3</sup>**

<sup>1</sup>Department of Manufacturing Engineering, Annamalai University, Annamalai Nagar-608002, Tamil Nadu, India

<sup>2</sup>Department of Manufacturing Engineering, Annamalai University, Annamalai Nagar-608002, Tamil Nadu, India

<sup>3</sup>Department of Mechanical Engineering, S R Gudlavalleru Engineering College, Gudlavalleru – 521356, Andhra Pradesh, India

## Abstract:

Aluminium 6061 (AA6061) plays an important role in modern engineering due to its versatile applications, including aerospace, automotive, and construction. This study explores AA6061 as a matrix material reinforced with walnut shell ash (WSA) and Silicon Carbide (SiC), produced through the ultrasonic-assisted stir casting technique. The research aims to improve the process parameters using the Taguchi L9 orthogonal array. The parameters include weight percentage of reinforcement - 2% (1%WSA+1%SiC), 4% (2%WSA+2%SiC), and 6% (3%WSA+3%SiC), Stirring speed (SS) - 300 rpm, 350 rpm, and 400 rpm, and Stirring time (ST) - 2, 3, and 4 minutes. The response properties examined are hardness, impact strength, and compressive strength. Optimal parameters for achieving maximum hardness are 6% reinforcement, 300 rpm stirring speed, and 2 minutes of stirring time. For optimal impact strength, the best conditions are 2% reinforcement, 300 rpm stirring speed, and 2 minutes of stirring time. For maximum compressive strength, the ideal parameters are 6% reinforcement, 400 rpm stirring speed, and 3 minutes of stirring time. Scanning Electron Microscope (SEM) images confirmed the uniform distribution of reinforcements, supporting the results. This study demonstrates the impact of optimizing process parameters to improve the mechanical properties of AA6061 composites, contributing significantly to their potential applications.

## ARTICLE HISTORY

Received: 24 September 2024

Revised: 25 November 2024

Accepted: 3 December 2024

Published: 16 December 2024

## KEYWORDS

AA6061 Alloy, Hybrid metal matrix nano composites, Stir casting parameters, Walnut shell ash, Mechanical properties

## 1. INTRODUCTION

Metal matrix composites (MMC's) have been tailored to meet the growing demands across various sectors, particularly in the manufacture of materials like connecting rods, braking systems, pistons, pins, and brake discs [1]. These composites are prized for their superior strength and tribological and mechanical properties. However, the widespread use of MMCs is often hindered by

challenges in their manufacturing processes [2]. Achieving optimal properties in these composites requires fine-tuning process parameters during fabrication. Several methods have been devised to produce MMCs, including the stir casting method, powder metallurgy (PM), centrifugal casting, vapor deposition method (VPD), and squeeze casting [3]. Among these, ultra sonic assisted stir casting method stands out due to its efficiency in large-scale production and relative simplicity [4].

Recently, carbon nanotubes (CNTs) have been explored as reinforcements for aluminum matrix composites, showcasing significant improvements in mechanical properties. For instance, CNT-reinforced Al-based composites developed via a modified flake powder metallurgy approach demonstrated enhanced wear resistance and tensile strength owing to the uniform distribution of CNTs within the matrix [5]. Additionally, structure-specific strengthening mechanisms in Al/graphene heterogeneous lamellar composites revealed that tailoring the reinforcement structure could significantly boost load-bearing capacity and energy dissipation, which is essential for high-stress applications [6]. Al-based nanocomposites fabricated using spark plasma sintering (SPS) highlighted the critical role of uniform dispersion and interfacial bonding in determining composite strength. The study underscored the influence of SPS parameters on microstructural refinement and mechanical performance [7]. Similarly, hot deformation behavior in bimodal-sized Al/Al<sub>2</sub>O<sub>3</sub> nanocomposites developed by SPS demonstrated enhanced ductility and strength due to improved particle-matrix interaction and grain refinement [8]. Advances in smart mechanical powder processing techniques have further optimized the production of carbon nanotube (CNT)-reinforced aluminum composites. These methods improve the dispersion of CNTs and minimize clustering, leading to superior mechanical properties such as increased hardness and reduced wear [9]. Integrating nano-sized reinforcements, such as SiC and walnut shell ash, into AA6061 alloys using stir casting has proven to enhance mechanical properties significantly. However, the interaction between reinforcement and matrix, coupled with the impact of process parameters like SS and ST, plays a decisive role in determining composite behavior.

The Taguchi method is frequently employed for optimizing process parameters because it effectively elucidates the interactions between these parameters [10]. Another common technique for assessing the significance and contribution of various input parameters to the desired responses is Analysis of variance (ANOVA) [11]. A variety of reinforcements, both harder and softer, are adopted to elevate the properties of the matrix material. Hard reinforcements namely SiC, TiB<sub>2</sub>, B<sub>4</sub>C, TiC, ZrO<sub>2</sub>, and TiO<sub>2</sub> are incorporated to boost the mechanical properties, while soft reinforcements like MoS<sub>2</sub> and Gr are used to reduce friction [12-16]. Reinforcing aluminum alloys like AA6061 with materials such as Silicon Carbide (SiC) significantly

enhances their mechanical properties, including hardness, tensile resistance, and wear resistance [17]. The stir casting method is well-regarded for its ability to produce metal matrix composites (MMCs) with consistent reinforcement distribution. Optimizing process parameters using methods like the Taguchi L9 orthogonal array is essential for achieving desired mechanical properties [18-20].

The wear of MMCs is largely affected by their micro-hardness, which is significantly improved with the addition of hard reinforcements [21]. This research aims to enhance the stir casting process parameters for AA6061-WSA-SiC metal matrix composites to improve their mechanical properties, such as microhardness, impact strength, and compressive strength. Despite extensive research on various MMCs, there has been limited exploration into the enhancement of process parameters specifically for AA6061-WSA-SiC composites. This research aims to fill that gap by identifying the optimal arrangement of stir-casting process parameters to maximize micro-hardness, impact, and compressive strength.

Aluminum alloys are widely recognized for their advantageous properties, such as excellent recyclability, superior resistance to corrosion, and exquisite thermal conductivity, which make them suitable for various engineering applications [22-24]. Furthermore, aluminum alloy composites and nanocomposites have found extensive use in sectors like aerospace, automotive, and marine industries due to their enhanced mechanical properties and weight reduction capabilities [25-26].

Recent advancements have introduced alternative production techniques, such as compocasting and thixoforming, which have demonstrated significant potential for manufacturing metal matrix composites. Compocasting, a semi-solid processing technique, offers improved particle dispersion and reduced porosity in composites [27-28]. Similarly, thixoforming, a semi-solid forming process, enables precise control of the microstructure, resulting in the improved mechanical performance of the final product [29-30]. These methods complement traditional stir casting by addressing its limitations and expanding the scope of aluminum-based composite fabrication. By integrating agro-waste-based reinforcements like walnut shell ash (WSA) with traditional hard reinforcements such as silicon carbide (SiC), this study not only enhances the mechanical properties of AA6061 alloy composites but also explores sustainable material solutions.

**2. MATERIALS AND METHODS**

In this research, aluminium alloy AA6061 was chosen as the matrix material. This alloy was selected due to its favourable properties and widespread use in various applications. The composition of AA6061 is detailed in the accompanying Table 1, highlighting its constituent elements. To enhance the mechanical properties of the composite material, walnut shell ash and silicon carbide were employed as reinforcing agents. Both reinforcements were selected for their ability to significantly enhance characteristics such as microhardness, impact strength, and compressive strength. The particle size of both silicon carbide and walnut shell ash was maintained between 60-80 nanometres to ensure uniform distribution and

effective reinforcement within the aluminium matrix. By incorporating these nano-sized reinforcements into the AA6061 matrix, the resultant composite is expected to exhibit superior mechanical performance, making it suitable for high-stress applications. The meticulous selection and combination of these materials aim to optimize the composite's overall structural integrity and durability. The walnut shell ash provides lightweight and low-cost reinforcement, while the silicon carbide enhances hardness and wear resistance [31,32]. Earlier studies have indicated that the inclusion of reinforcements like zircon sand, tungsten carbide, and boron carbide can contribute to a rise in tensile and compressive strength of aluminium alloys up to an optimal reinforcement percentage, beyond which the properties may decline [33].

**Table 1.** Elements in AA6061 alloy

Element	Mg	Si	Fe	Cu	Mn	Zn	Ti	Cr	Al
Composition	0.8 -1.2	0.4 -0.8	0.0 -0.7	0.15 -0.40	0.0 -0.15	0.0 -0.25	0.0 -0.25	0.04 -0.35	Balance

**2.1 Preparation of Reinforcement**

Walnut shells are meticulously washed to eliminate any impurities, including dirt, dust, and leftover organic substances. This washing procedure guarantees that the walnut shells are devoid of any elements that might impact the characteristics of the ash. The washed shells are then dried to remove any traces of moisture, making sure they are thoroughly dry before proceeding with further steps. The dried shells are then heated in a furnace to transform them into ash. Following the heating, the ash is allowed to cool naturally to room temperature to avoid any sudden changes that could affect the ash's properties. The cooled ash is then pulverized into a fine powder using a ball milling technique. This step is essential to reach the desired particle size, which is usually between 60-80 nm for the best reinforcement in metal matrix composites. The ball milling process was conducted at a rotational speed of 250 rpm for a duration of 20 hours using tungsten carbide balls as the grinding medium. This setup ensured effective size reduction and uniformity of the particles. Following the ball milling, sieving was performed to maintain consistency and particle size analysis was carried out to verify that the desired size range was achieved. These controlled

parameters were crucial for ensuring the uniform dispersion of reinforcements within the AA6061 matrix, thereby enhancing the mechanical properties of the composite. The powdered ash is then sifted to ensure an even distribution of particle sizes. The prepared walnut shell ash is stored in airtight containers to keep it free from contamination and moisture absorption. Additionally, silicon carbide reinforcement material of the same particle size was procured.

**2.2 Fabrication of Hybrid Aluminium Metal Matrix Nanocomposites**

In this study, a stir-casting technique assisted by ultrasonic waves was used to accomplish a consistent dispersion of matrix and reinforcement particles. The focus was on addressing concerns such as preventing the bottom of the graphite crucible from drying out and ensuring an even distribution of SiC, WSA, and reinforcement particles in the molten metal. The alloy AA6061 is shaped into round rods, which are then cut into numerous smaller units. A limited no. of these rod pieces is placed in the crucible furnace. To elevate the interaction between the reinforcement and matrix, a 1% magnesium additive is used to improve the material's wettability. Additionally, a

deoxidizing agent is employed to avert oxidation during the casting process [34]. The reinforcement is preheated for 2 hours at 350°C. The process for creating AA6061-WSA-SiC composites involves varying the parameters of the stir casting technique, including the reinforcement weight percentage - 2% (1% WSA + 1% SiC), 4% (2% WSA + 2% SiC), and 6% (3% WSA + 3% SiC), SS (300, 350, and 400 rpm), and ST (2, 3, and 4 min). The reinforcement particles are initially set in a furnace and heated to the target temperature. They are then preheated for 2 hours at 350°C [35]. After preheating, the reinforcement is added to the furnace, and the stirrer is run at the specified speed for a set amount of time. During the stir-casting process, ultrasonic waves were applied using a high-frequency ultrasonic probe. The frequency of the ultrasonic waves was maintained at 20 kHz with a power output of 2 kW. This ultrasonic treatment was applied continuously during the stirring phase to ensure uniform distribution of the reinforcement particles within the molten AA6061 matrix. The use of ultrasonic waves aids in breaking up agglomerates and enhances the wetting of the reinforcements, leading to improved mechanical properties. The cast is then prepared by dispensing the molten metal into the mold which is preheated to 250°C.

This procedure is applied multiple times using different sets of process parameters. A total of 9 specimens were produced at 9 different process parameter settings, the input variables and levels are shown in Table 2, and the L9 orthogonal array combination process parameters are detailed in Table 3. The composite castings were air-cooled after removal from the mold. To further enhance the material properties and alleviate residual stresses, the castings were placed in a furnace for 6 hours at a temperature of 200°C. This heat treatment process helped reduce internal stresses and improve the overall structural integrity of the composite. The resulting composite had a diameter of 15 mm and a length of 250 mm.

**Table 2.** Input variables and their levels

Levels	Percentage of Reinforcement (wt%) (A)	Stirring Speed (SS) (B)	Stirring Time (ST) (C)
	%	rpm	minutes
1	2	300	2
2	4	350	3
3	6	400	4

**Table 3.** Process parameter combinations for experimental design

Experiment No.	Input Variables		
	wt(%)	SS (rpm)	ST (minutes)
E1	2	300	2
E2	2	350	3
E3	2	400	4
E4	4	300	3
E5	4	350	4
E6	4	400	2
E7	6	300	4
E8	6	350	2
E9	6	400	3

In this study, the Taguchi L9 orthogonal array was employed to optimize the process parameters efficiently. The use of the Taguchi method minimizes the number of experiments required, thereby reducing both time and cost while providing a comprehensive understanding of how each parameter affects the desired outcomes. This approach allows for the effective optimization of multiple factors with a limited set of experiments. In addition to the Taguchi method, other multi-optimization techniques are gaining traction to enhance the accuracy and reliability of experimental results further. Techniques such as the Taguchi Grey Relational Analysis (GRA), TOPSIS (Technique for Order of Preference by Similarity to Ideal Solution), and Artificial Neural Networks (ANN) are frequently employed in multi-response optimization scenarios [36]. These methods are particularly useful when multiple output responses need to be optimized simultaneously, offering better decision-making capabilities in complex manufacturing processes [37]. The influence of multi-objective optimization techniques on composite materials, emphasizing their role in improving mechanical properties through efficient parameter selection. The authors demonstrate the effectiveness of using advanced optimization methods to reduce experimental trials while achieving high-performance material properties. This work highlights the practical benefits of combining computational tools with experimental approaches for composite design [38]. While the Taguchi L9 orthogonal array is utilized for the current optimization of mechanical properties such as micro-hardness, impact resistance, and compressive strength, future work will incorporate multi-criteria optimization techniques such as Taguchi Grey Relational Analysis (GRA) to address additional response variables. This will allow for a

more robust understanding and optimization of the composite material properties, further enhancing its potential applications in various engineering fields.

### 2.2.1 Response-to-Noise (SNR) Ratio

The Response-to-Noise (SNR) ratio is a statistical metric used in process optimization to evaluate the quality of output responses while minimizing variability. It is derived from the Taguchi method, a robust design approach aimed at improving process performance and product quality. The S/N ratio quantifies the degree to which a process parameter influences the desired output by considering both the mean and the variability of the response [39]. This ensures a balance between achieving the target output and minimizing the impact of uncontrollable external factors (noise).

Three key characteristics of the S/N ratio are typically recognized, depending on the desired:

**Smaller-is-Better** - Used when the objective is to minimize the response value:

$$S/N = -10 \log \left( \frac{1}{p} \sum_{i=1}^p a_i^2 \right), \quad (1)$$

where is:  $a_i$  - observed response value.

**Nominal-is-Best** - Applied when achieving a specific target value is critical:

$$S/N = -10 \log \left( \frac{\bar{a}}{s^2} \right), \quad (2)$$

where are:  $\bar{a}$  - is the mean,  $s^2$  - is the variance of the response.

**Larger-is-Better** - Utilized when maximizing the response value is desired:

$$S/N = -10 \log \left( \frac{1}{p} \sum_{i=1}^p \frac{1}{a_i^2} \right). \quad (3)$$

## 2.3 Evaluation of Mechanical Properties

### 2.3.1 Micro Hardness Test

Hardness measures a material's indentation resistance, often assessed using the Vickers microhardness test [40]. In the current study, the Vickers micro-hardness test was conducted on aluminium hybrid nano-composite samples. The testing was carried out in accordance with ASTM E384 standards [41], applying a load of 100 g and a dwell period of 10 seconds. Samples were polished, and the microhardness readings were taken at four different locations, with the average values reported.

### 2.3.2 Impact Test

The Charpy impact test is a dependable technique used to measure the energy absorbed by a material during fracture when impacted by a pendulum [42]. In this study, a Charpy V-notch specimen with a height of 55 mm, a square cross-section of 10×10 mm, and a notch depth of 2 mm was utilized. Impact strength readings were taken from 3 samples for each combination, and the average values were reported.

### 2.3.3 Compressive Strength

In this study, Standardized test methods, such as axial crushing tests, are typically used to measure the crushing strength of a material. The tests were conducted using a 400 kN Universal Testing Machine, with specimens prepared to a standard size of 6.35 mm in radius and 25.4 mm in height. Compressive strength readings were taken from 3 samples for each combination, and the average values were reported.

## 3. RESULTS AND DISCUSSION

The AA6061-WSA-SiC composites were fabricated using the Taguchi L9 orthogonal array, which enabled a systematic variation of the process parameters in the stir-casting technique. This method allowed the evaluation of multiple input parameter combinations to enhance the properties of the composites. Following the fabrication process, the composite samples were subjected to several tests, such as the Vickers microhardness test, impact test, and compression test, to determine their mechanical performance. In this study, the optimal parameters were identified through the use of the Taguchi L9 orthogonal array, which helped in minimizing the number of experimental runs required while still covering a wide range of parameter combinations. This approach not only reduced both time and cost but also allowed for an in-depth examination of the interactions between critical process parameters, including the percentage of reinforcement, stirring speed, and stirring time. The influence of these parameters on the mechanical properties, such as hardness, impact strength, and compressive strength, was thoroughly analyzed. Additionally, the methodology applied signal-to-noise (SNR) analysis under the "larger-is-better" criterion, which helped identify the optimal combination of parameters to maximize the desired outcomes. This

statistical approach ensured a balanced experimental setup, highlighting the influence of each individual parameter while considering their combined effects on the overall mechanical properties of the composites.

The use of the L9 orthogonal array enables a comprehensive analysis of how each stir-casting parameter influences the final properties of the composites. This method ensures a balanced and efficient evaluation process by covering a wide range of parameter combinations with a minimal number of experiments. The optimization of these parameters is critical to enhancing the overall performance of the composites. Minitab 19

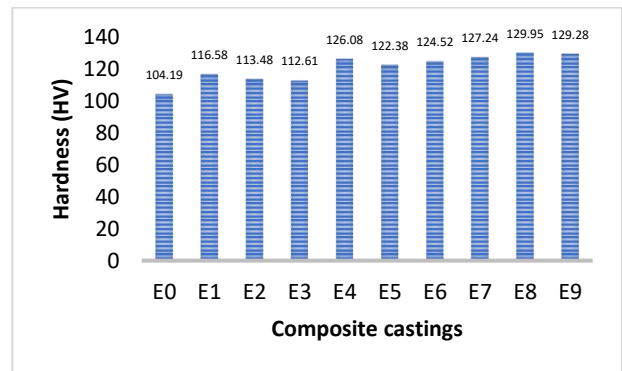
software is utilized to achieve this optimization. This statistical software helps analyse the data obtained from the tests, allowing for the identification of the most significant factors affecting the composite's properties. Through this analysis, the optimal set of process parameters can be determined, leading to the production of composites with superior mechanical characteristics. By employing this systematic and analytical approach, the study aims to maximize the potential of AA6061-WSA-SiC composites in various engineering applications, ensuring they meet the necessary performance standards. The output responses and S/N ratio values are presented in Table 4.

**Table 4.** Output response and the response-to-noise ratio (SNR) (larger the better)

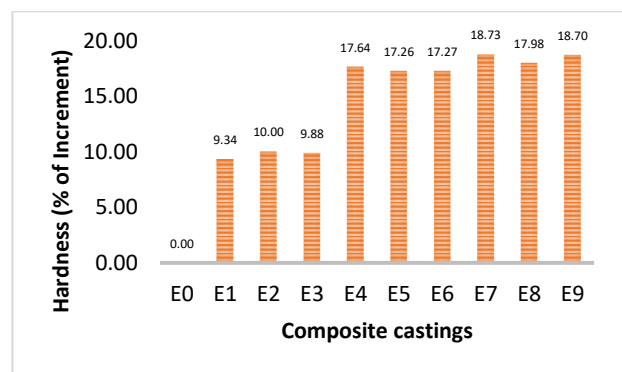
Experiment No	Output response			S/N Ratio		
	Hardness (HV)	Impact Strength (J/mm <sup>2</sup> )	Compressive Strength (N/mm <sup>2</sup> )	Hardness	Impact Strength	Compressive Strength
E1	116.58	0.525	270.67	41.3325	-5.59681	48.6489
E2	113.48	0.500	272.32	41.0984	-6.02060	48.7016
E3	112.61	0.479	272.02	41.0312	-6.39027	48.6920
E4	126.08	0.483	291.23	42.0126	-6.31507	49.2848
E5	122.38	0.458	290.28	41.7544	-6.77637	49.2564
E6	124.52	0.465	290.32	41.9046	-6.65873	49.2576
E7	127.24	0.454	293.93	42.0925	-6.85569	49.3650
E8	129.95	0.438	292.06	42.2754	-7.18044	49.3095
E9	129.28	0.442	293.85	42.2308	-7.09811	49.3624

### 3.1 Microhardness

The microhardness of AA6061 hybrid metal matrix composites (HMMC), reinforced with WSA and SiC, was evaluated under various processing parameters, including reinforcement weight percentage, stirring speed, and stirring time. The bar charts in Figs. 1(a)-1(b), illustrate significant variations in hardness across the different experimental conditions. An increase in both the reinforcement percentage and stirring parameters resulted in improved hardness. In Experiment E7, the highest hardness value was recorded at 127.24 HV with 6% reinforcement, a SS of 300 rpm, and a ST of 4 min. Experiment E8, with a SS of 350 rpm and a reduced ST of 2 min, further enhanced the hardness to 129.95 HV. This indicates that higher reinforcement percentages and optimal stirring conditions positively affect the mechanical properties of the composite material. Conversely, the lowest hardness value of 112.61 HV occurred in Experiment E3, which involved 2% reinforcement, a SS of 400 rpm, and a ST of 4 min. This reduction in hardness at higher stirring speeds, especially with lower reinforcement levels, may be due to poor particle distribution or clustering during processing.



(a)



(b)

**Fig. 1.** (a) Hardness Values of Composites; (b) Hardness (% of Increment) Values of Composites

The percentage increase in hardness closely mirrored the absolute hardness values, with the maximum percentage increase (24.72%) observed in Experiment E8 (6% reinforcement, 350 rpm, 2 minutes), and the lowest increase (8.08%) seen in Experiment E3 (2% reinforcement, 400 rpm, 4 minutes). These findings suggest that an optimal balance of reinforcement percentage and processing parameters significantly enhances the material's mechanical performance.

Fig. 2 presents the main effect plot for Vickers microhardness as it relates to response-to-noise ratio (SNR), with the associated data provided in Table 5. For optimizing the process parameters of stir casting to enhance microhardness, the "larger is better" criterion was applied [11]. This analysis revealed that increasing the amount of reinforcement leads to higher microhardness in AA6061-WSA-SiC composites, with the maximum microhardness achieved at 6 wt% reinforcement (A3). SS emerged as a crucial parameter for achieving an even distribution of reinforcement within the AA6061 matrix. Microhardness increased as the SS rose from 300 rpm-350 rpm but declined at 400 rpm. Thus, the maximum microhardness was observed at an SS of 350 rpm (B2). ST also significantly impacted the microhardness of the composites. Microhardness improved as ST increased from 2 to 3 minutes but decreased at 4 minutes. The highest hardness value was recorded at an ST of 2 minutes (C1).

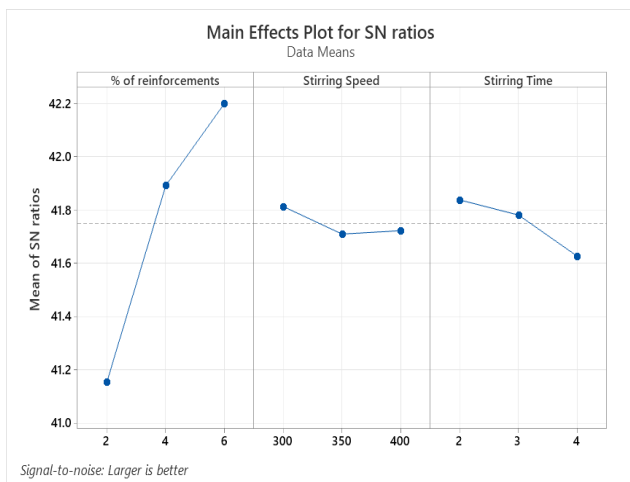


Fig. 2. Main effect plot for the response-to-noise ratio (SNR) of microhardness

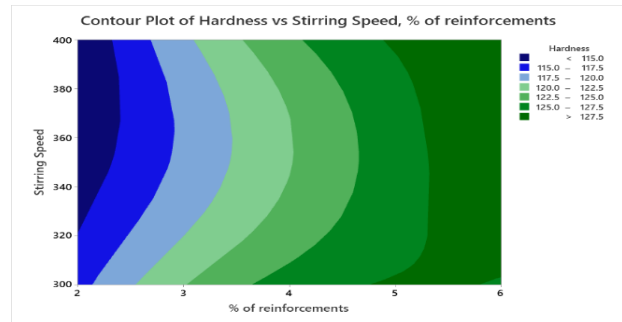
The response table shows that the order of influence of input process parameters on the microhardness of AA6061-WSA-SiC composites is wt%, SS, and ST. From the main effect plot analysis, the superior combination of input variables is identified as 6 wt% reinforcement, an ST of

2 minutes, and an SS of 300 rpm, designated as A3B1C1.

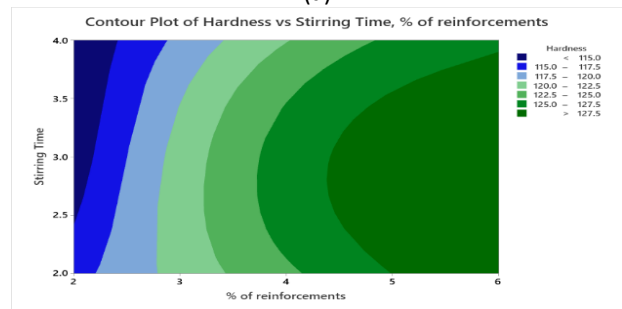
The Isoline plots for micro-hardness are illustrated in Figs. 3(a)–3(c). These plots analyze the interactions between various combinations of input parameters: wt% and SS, wt% and ST, and ST and SS. The analysis shows that all input process parameters influence microhardness, as evidenced by the intersection of all parameters with each other.

Table 5. Response table for the SNR (larger the better)

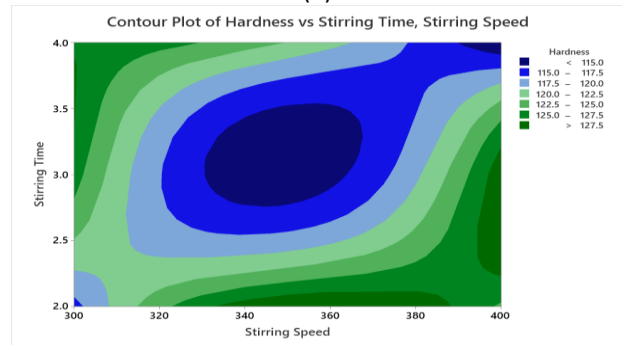
Levels	wt% of reinforcements	SS	ST
1	41.15	41.81	41.84
2	41.89	41.71	41.78
3	42.20	41.72	41.63
Delta	1.05	0.10	0.21
Rank	1	3	2



(a)



(b)



(c)

Fig. 3. (a) Isoline plots of micro-hardness with SS, wt% of Reinforcements; (b) Isoline plots of micro-hardness with ST, wt% of Reinforcements; (c) Isoline plots of micro-hardness with ST, SS

### 3.2 Impact Strength

The impact strength of AA6061 hybrid composites reinforced with walnut shell ash (WSA) and silicon carbide (SiC) was evaluated under different processing conditions, including varying the reinforcement weight percentage, stirring speed (SS), and stirring time (ST). The results are presented in the bar charts Figs. 4(a)-4(b) reveals significant trends in the behavior of impact strength based on these parameters. The results indicate that the impact strength tends to decrease as the reinforcement percentage increases. Experiment E1, with 2% reinforcement, an SS of 300 rpm, and an ST of 2 min, attained the highest impact resistance of 0.533 J/mm<sup>2</sup>. In contrast, Experiment E9, which used 6% reinforcement, an SS of 400 rpm, and an ST of 3 min, showed the lowest impact strength at 0.438 J/mm<sup>2</sup>. This reduction in impact strength with increased reinforcement content is likely due to the brittle nature of the WSA and SiC particles, which lowers the ductility of the composite matrix. Further, it was observed that higher stirring speeds and extended stirring times negatively affected the impact strength. For instance, in Experiment E3, which had 2% reinforcement, a stirring speed of 400 rpm, and a stirring time of 4 minutes, the impact strength dropped to 0.5 J/mm<sup>2</sup>. A similar reduction was noted in Experiment E8 (6% reinforcement, 350 rpm, 2 minutes), where the impact strength decreased to 0.454 J/mm<sup>2</sup>. These findings suggest that while the addition of reinforcements strengthens the composite's hardness, it simultaneously reduces its ability to absorb energy under impact.

The percentage decrement in impact strength exhibited a similar trend. Experiment E1, which showed the highest impact strength, correspondingly had the smallest percentage decrement at 1.50%. On the other hand, Experiment E8 demonstrated the largest percentage decrement of 17.82%, closely followed by Experiment E9 at 17.07%. This trend underscores the fact that higher reinforcement percentages contribute to a decline in material toughness, making the composite more prone to fracture when subjected to impact forces. The findings indicate that achieving an optimal balance between the reinforcement percentage and processing parameters is crucial to ensuring the composite maintains both adequate mechanical strength and toughness. While increasing reinforcement percentages may improve other mechanical

properties, such as hardness, this comes at the expense of impact strength. Therefore, careful selection of reinforcement content and process conditions is necessary for applications where both hardness and impact resistance are important considerations.

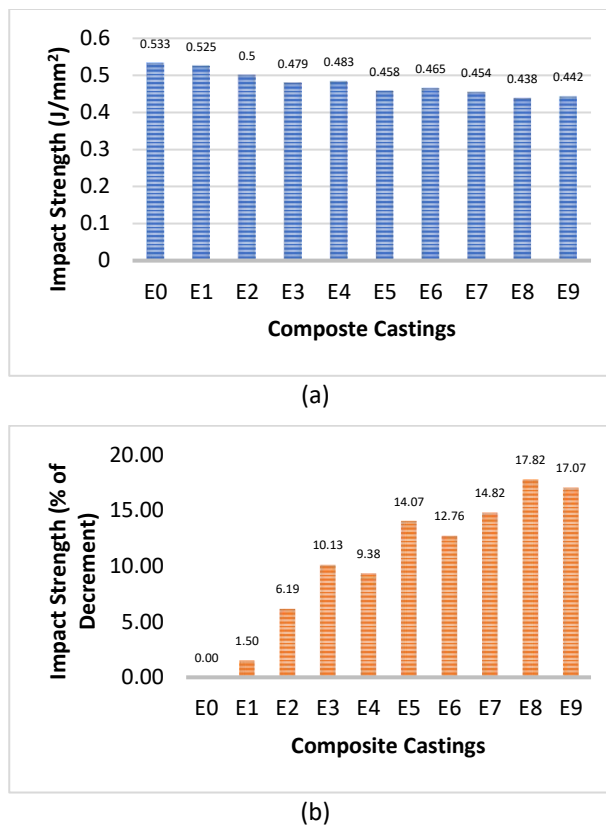


Fig. 4. (a) Impact Strength Values of Composites; (b) Impact strength (% of Decrement) Values of Composites

The main effect plot for the response-to-noise ratio (SNR) of impact strength is illustrated in Fig. 5, with the relevant data summarized in Table 6. To optimize the stir-casting process parameters for enhancing impact strength, the "larger is better" criterion was utilized. This analysis showed that increasing the amount of reinforcement actually decreases the impact strength of AA6061-WSA-SiC composites, with the highest impact strength achieved at 2 wt% reinforcement (A1). SS was identified as a critical parameter for ensuring the even distribution of the reinforcement within the AA6061 matrix. The impact strength was highest at an SS of 300 rpm (B1) and declined with the rise in speed from 300 to 400 rpm. ST also played a significant role in affecting the impact strength of the composites. The impact strength was found to be highest with an ST of 2 minutes (C1) and decreased when the ST was extended to 4 minutes.

**Table 6.** Response table for the SNR (larger the better)

Levels	wt% of reinforcements	SS	ST
1	-6.003	-6.256	-6.479
2	-6.583	-6.659	-6.478
3	-7.045	-6.716	-6.674
Delta	1.042	0.460	0.196
Rank	1	2	3

The response table reveals that the order of effect of the input process parameters on the impact strength of AA6061-WSA-SiC composites is as follows: wt%, ST, and SS. According to the main effect plot, the superior combination of input process variables is determined to be 2 wt% reinforcement, an SS of 300 rpm, and an ST of 2 minutes, signified as A1B1C1.

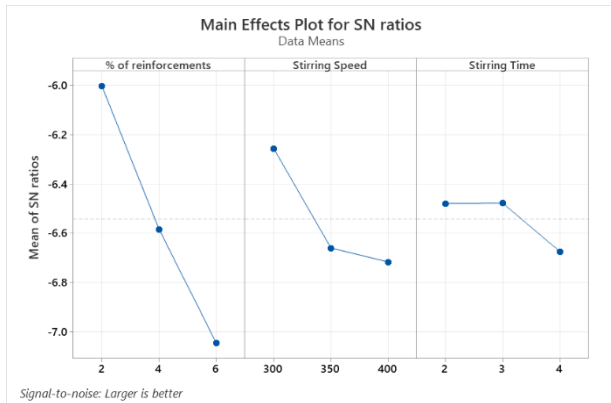
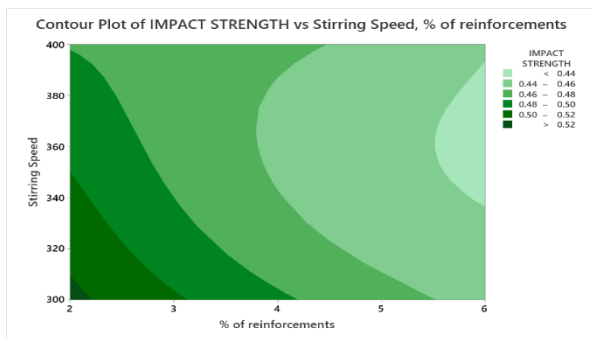
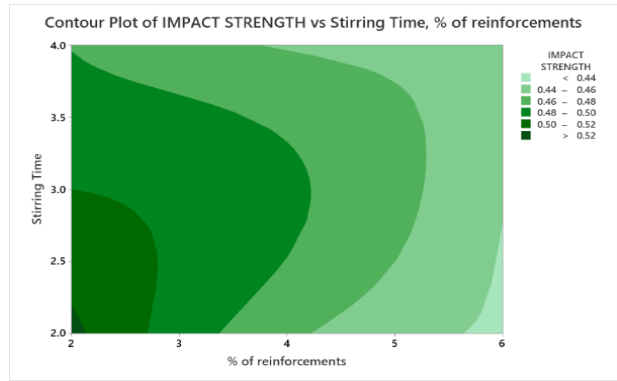


**Fig. 5.** Main effect plot for the response-to-noise ratio (SNR) of impact strength

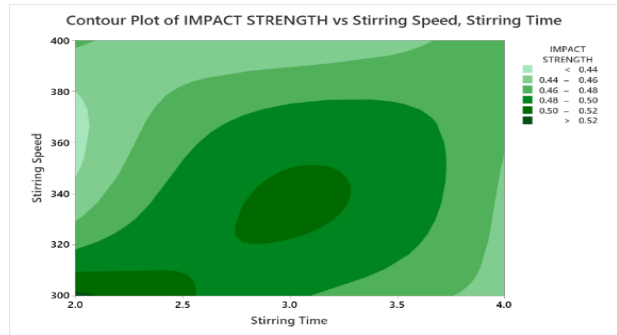
The Isoline plots for impact strength are depicted in Figs. 6(a)–6(c). These plots examine the interactions between different combinations of input parameters: wt% and SS, wt% and ST, and ST and SS. The analysis indicates that all input process parameters affect impact strength, as shown by the intersections of these parameters with each other.



(a)



(b)



(c)

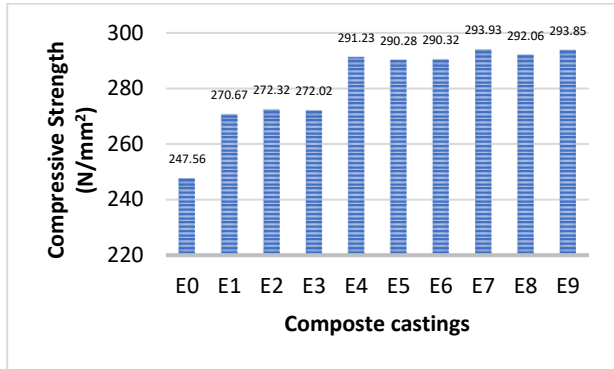
**Fig. 6.** (a) Isoline plots of impact strength with SS, wt% of Reinforcements; (b) Isoline plots of impact strength with ST, wt% of Reinforcements; (c) Isoline plots of impact strength with ST, SS

### 3.3 Compressive Strength

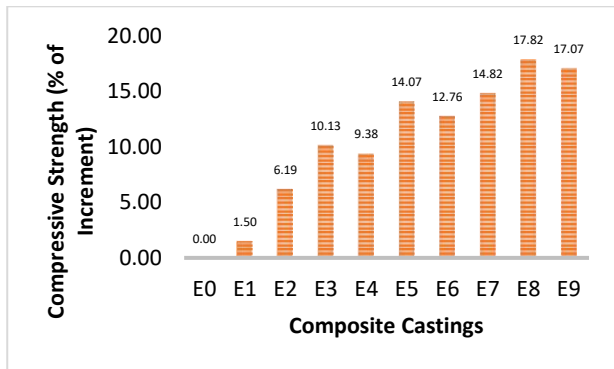
The study evaluated the influence of varying stirring speeds (SS), stirring times (ST), and weight percentages (Wt%) on the compressive strength of composites. The results, presented in Figs. 7(a)-7(b), reveal significant trends in the mechanical properties. The compressive strength increased with higher weight percentages of the reinforcing material. For a weight percentage of 6%, the maximum compressive strength was observed at 293.93 N/mm<sup>2</sup> (E7) with an SS of 300 rpm and an ST of 4 min. Comparatively, lower compressive strength values were recorded for a weight percentage of 2%, where the highest value was 272.32 N/mm<sup>2</sup> (E2) at an SS of 350 rpm and an ST of 3 min.

The percentage increment in compressive strength also demonstrated similar patterns. The maximum increment of 18.73% was achieved with 6% weight reinforcement (E7), while the minimum of 9.34% was recorded with 2% weight reinforcement (E1). These findings indicate that an increase in weight percentage positively influences mechanical strength, albeit with varying effects based on stirring speed and time. The stirring speed and time played a crucial role in determining the

uniformity and quality of the composite structure. For instance, moderate stirring speeds (350 rpm) and times (3-4 minutes) provided optimal results, as seen in E5 and E7. Conversely, extreme stirring conditions, such as low stirring speed (300 rpm) with reduced stirring time (2 minutes), resulted in suboptimal strength, as shown in E8.



(a)



(b)

Fig. 7. (a) Compressive Strength Values of Composites; (b) Compressive strength (% of Increment) Values of Composites

The primary impact graph for the response-to-noise (SNR) of the crushing strength is depicted in Fig. 8, with the pertinent information outlined in Table 7. To fine-tune the stir casting procedure for boosting the compressive strength, the principle of "larger is better" was applied. This examination revealed that adding more reinforcement actually enhances the compressive strength of AA6061-WSA-SiC composites, with the peak compressive strength observed at 6 wt% reinforcement (A3). The stirring speed was identified as a crucial factor in achieving Consistent reinforcement spread in the AA6061 matrix. The peak compressive strength was reached at an SS of 300 rpm (B1), and it decreased as the SS rose from 350 to 400 rpm. The duration of stirring also had a significant impact on the compressive strength of the composites. The peak compressive strength was observed with a ST of 4 minutes (C3), and it decreased with ST's shorter than 2 minutes.

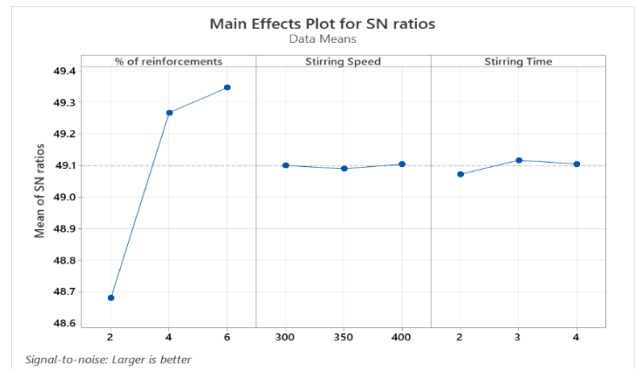
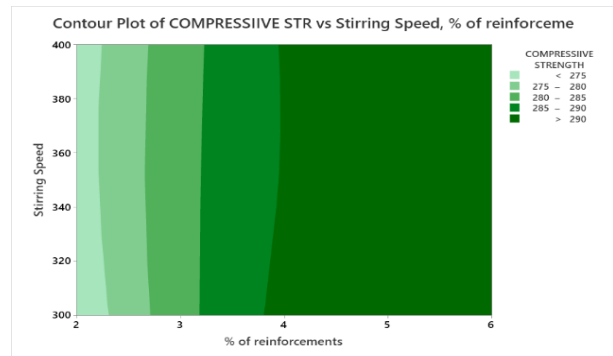


Fig. 8. Main effect plot SNR for compressive strength

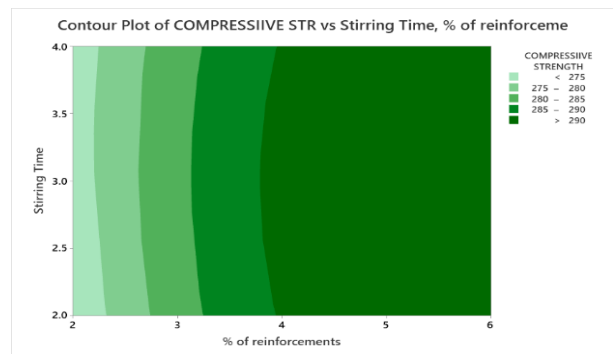
Table 7. Response table for response-to-noise ratio (SNR) (larger the better)

Levels	wt% of reinforcements	SS	ST
1	271.7	285.3	284.4
2	290.6	284.9	285.8
3	293.3	285.4	285.4
Delta	21.6	0.5	1.4
Rank	1	3	2

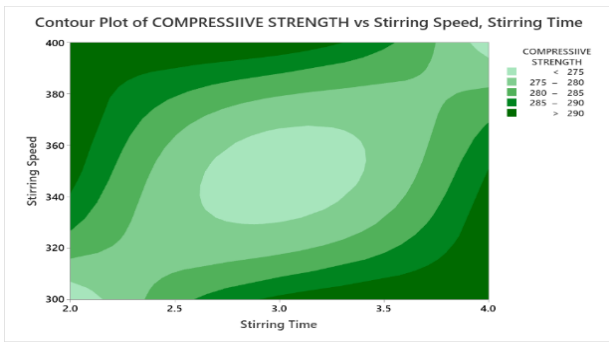
Figs. 9(a)–9(c) display the Isoline plots for compressive strength, illustrating the interactions between different combinations of input parameters: wt% and SS, wt% and ST, and ST and SS. The analysis demonstrates that all input process parameters affect compressive strength, as evidenced by the intersections among these parameters.



(a)



(b)



(c)

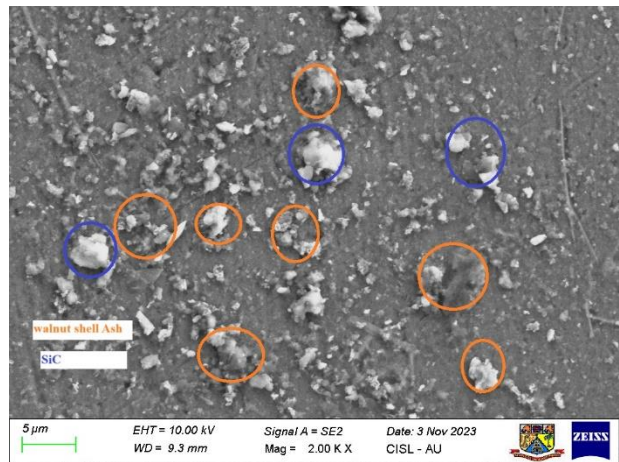
**Fig. 9.** (a) Isoline plots of compression strength with SS, Reinforcements percentages; (b) Isoline plots of compression strength with ST, Reinforcements percentages; (c) Isoline plots of compression strength with SS, ST

### 3.4 SEM Analysis

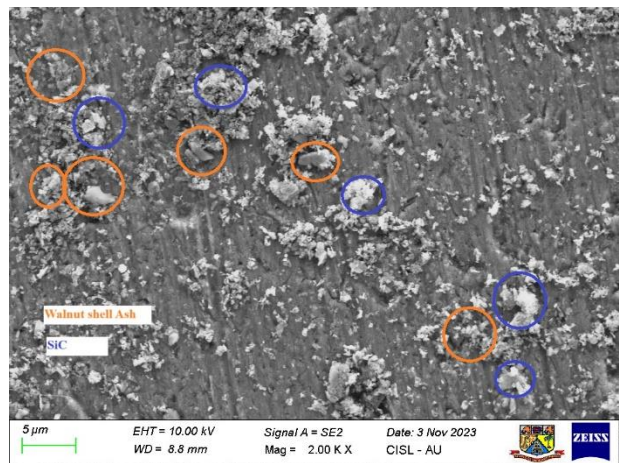
The Scanning Electron Microscopy (SEM) analysis provided crucial insights into the microstructural characteristics of the AA6061-Walnut Shell Ash (WSA)-Silicon Carbide (SiC) composites. The even dispersion of WSA and SiC particles within the aluminum matrix, as evident in SEM images shown in Figs. 10(a)-10(c) played a pivotal role in enhancing the mechanical properties. This uniform distribution minimizes the formation of agglomerates and ensures effective Load dispersion through the matrix and reinforcements.

The enhancement in microhardness can be attributed to the hard, brittle nature of the reinforcement particles, which act as obstacles to dislocation movement within the matrix. The SEM images revealed the absence of significant voids or clusters, indicating that the stirring parameters were effective in achieving homogeneous particle dispersion. The improved compressive strength is a direct result of the effective load-bearing capacity of the reinforcements. The SEM analysis showed that the reinforcing particles were well-integrated with the matrix, providing strong interfacial bonding. This integration restricts the plastic deformation of the matrix under compressive loads, enhancing its strength. Furthermore, the small particle size and uniform distribution of WSA and SiC aid in the even distribution of stress across the composite, reducing the likelihood of localized failure. Despite the enhancements in hardness and compressive strength, the SEM analysis suggests a trade-off in impact strength due to the increased brittleness introduced by the reinforcements. The uniform dispersion of particles ensures structural integrity; however, the inherent brittleness of the SiC and WSA particles reduces the matrix's ability to

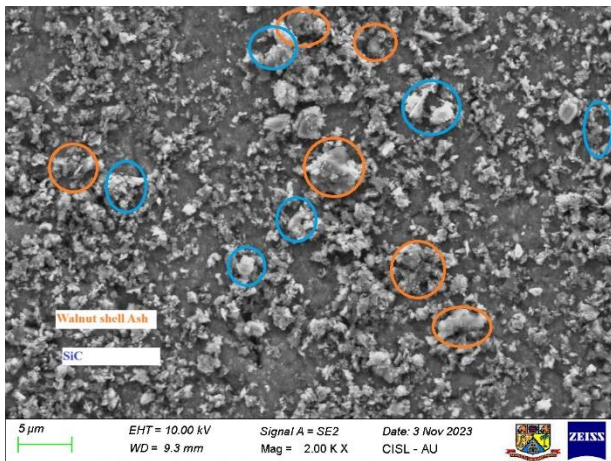
absorb energy during impact. The SEM micrographs showed no significant cracks or voids, confirming that the decrease in impact resistance is primarily due to the brittle nature of the reinforcements rather than processing flaws. The optimal stirring speeds and times used during the fabrication process ensured adequate wetting of the reinforcement particles by the molten aluminum. This wetting is evident in the SEM images, where a clear, continuous interface between the matrix and reinforcements is observed. This strong interface is essential for mechanical performance, as it facilitates efficient stress transfer and prevents premature failure at the particle-matrix boundaries. The SEM findings underscore the importance of microstructural uniformity in determining the mechanical behavior of composites. These observations validate the choice of process parameters and reinforce the critical role of reinforcement dispersion in achieving superior composite properties.



(a)



(b)



(c)

Fig. 10. (a) SEM image of Experiment 2 (b) SEM image of Experiment 5. (c) SEM image of Experiment 7

#### 4. CONCLUSION

The study effectively optimized the mechanical properties of AA6061 composites reinforced with walnut shell ash (WSA) and silicon carbide (SiC) by fine-tuning stir-casting process parameters using the Taguchi L9 orthogonal array. The investigation identified the following optimal conditions: a maximum hardness of 129.95 HV at 6% reinforcement, 350 rpm stirring speed, and 2 minutes stirring time; the highest notched impact strength of 0.533 J/mm<sup>2</sup> achieved at 2% reinforcement, 300 rpm stirring speed, and 2 minutes stirring time; and a peak compressive strength of 293.93 N/mm<sup>2</sup> at 6% reinforcement, 300 rpm stirring speed, and 4 minutes stirring time.

The Scanning Electron Microscopy (SEM) analysis confirmed a uniform dispersion of reinforcement particles, which contributed to enhanced microhardness and compressive strength. However, the increased reinforcement content led to a reduction in impact strength, attributed to the brittleness of the reinforcements. These findings highlight the significance of balancing reinforcement content and process parameters to achieve desired mechanical properties. The optimized AA6061-WSA-SiC composites demonstrate potential for high-performance engineering applications, offering a balance of strength, durability, and lightweight characteristics. A key limitation of this study is the potential variability in the uniform distribution of reinforcements, particularly walnut shell ash (WSA) and silicon carbide (SiC), within the AA6061 matrix. Although the ultrasonic-assisted stir-casting process was employed to promote uniform dispersion, minor inconsistencies in particle

distribution could still occur, especially at higher reinforcement percentages. This variability may lead to localized differences in mechanical properties, such as hardness and compressive strength, across different samples. Furthermore, this limitation affects the reproducibility of the results, as achieving the same level of uniformity in reinforcement dispersion across different batches may prove challenging. Future research should focus on refining the ultrasonic stirring parameters or exploring alternative methods to ensure more consistent particle distribution, which would enhance the reliability and scalability of the process for industrial applications. Additionally, future studies could investigate properties such as wear resistance, density, and fatigue strength to provide a more comprehensive evaluation of the composite materials. Employing techniques like Grey Relational Analysis for multi-objective optimization would allow simultaneous optimization of these mechanical and physical properties, ensuring a balanced and robust performance for diverse engineering applications.

#### CONFLICTS OF INTEREST

The authors declare no conflict of interest.

#### REFERENCES

- [1] J. Hirsch, Aluminium in Innovative Light-Weight Car Design. *Materials Transactions*, 52(5), 2011: 818–824. <https://doi.org/10.2320/matertrans.l-mz201132>
- [2] C.O. Ujah, D.V.V. Kallon, Trends in Aluminium Matrix Composite Development. *Crystals*, 12(10), 2022: 1357. <https://doi.org/10.3390/cryst12101357>
- [3] C.S. Shyn, R. Rajesh, M.D. Anand, Review of aluminium 6061 metal matrix composites fabricated using stir casting method and applications. *AIP Conference Proceedings*, 2317, 2021: 030027. <https://doi.org/10.1063/5.0036169>
- [4] U.K.G.B. Annigeri Veeresh Kumar, Method of stir casting of Aluminum metal matrix Composites: A review. *Materials Today Proceedings*, 4(2), 2017: 1140–1146. <https://doi.org/10.1016/j.matpr.2017.01.130>
- [5] B. Sadeghi, P. Cavaliere, CNTs reinforced Al-based composites produced via modified flake powder metallurgy. *Journal of Materials Science*, 57(4), 2022: 2550–2566. <https://doi.org/10.1007/s10853-021-06665-9>

- [6] B. Sadeghi, P. Cavaliere, C.I. Pruncu, Architecture dependent strengthening mechanisms in graphene/Al heterogeneous lamellar composites. *Materials Characterization*, 188, 2022: 111913. <https://doi.org/10.1016/j.matchar.2022.111913>
- [7] P. Cavaliere, B. Sadeghi, M. Shamanian, F. Ashrafizadeh, Al-Based Nanocomposites Produced via Spark Plasma Sintering: Effect of Processing Route and Reinforcing Phases. In: P. Cavaliere, (eds) *Spark Plasma Sintering of Materials*. Springer, Cham, 2019: 161–190. [https://doi.org/10.1007/978-3-030-05327-7\\_6](https://doi.org/10.1007/978-3-030-05327-7_6)
- [8] B. Sadeghi, P. Cavaliere, M. Nosko, V. Trembošová, S. Nagy, Hot deformation behaviour of bimodal sized Al<sub>2</sub>O<sub>3</sub>/Al nanocomposites fabricated by spark plasma sintering. *Journal of Microscopy*, 281(1), 2020: 28–45. <https://doi.org/10.1111/jmi.12947>
- [9] B. Sadeghi, G. Fan, Z. Tan, Z. Li, A. Kondo, M. Naito, Smart Mechanical Powder Processing for Producing Carbon Nanotube Reinforced Aluminum Matrix Composites. *KONA Powder and Particle Journal*, 39, 2021: 219–229. <https://doi.org/10.14356/kona.2022004>
- [10] T.K. Ibrahim, D.S. Yawas, B. Dan-asabe, A.A. Adebisi, Taguchi optimization and modelling of stir casting process parameters on the percentage elongation of aluminium, pumice and carbonated coal composite. *Scientific Reports*, 13, 2023: 2915. <https://doi.org/10.1038/s41598-023-29839-8>
- [11] S. Deshmukh, A. Ingle, D. Thakur, Optimization of stir casting process parameters in the fabrication of aluminium based metal matrix composites. *Materials Today Proceedings*, 2023. <https://doi.org/10.1016/j.matpr.2023.08.023>
- [12] X. Liao, L. Gao, X. Wang, F. Zhang, L. Liu, L. Ren, Mechanical properties of Boron Carbide/Reduced-Graphene-oxide composites Ceramics. *Journal of Wuhan University of Technology-Mater. Sci. Ed.*, 37(6), 2022: 1087–1095. <https://doi.org/10.1007/s11595-022-2638-4>
- [13] S. Gudipudi, S. Nagamuthu, K.S.Subbian S.P.R. Chilakalapalli, Enhanced mechanical properties of AA6061-B<sub>4</sub>C composites developed by a novel ultra-sonic assisted stir casting. *Engineering Science and Technology an International Journal*, 23(5), 2020:1233–1243. <https://doi.org/10.1016/j.jestch.2020.01.010>
- [14] H. Mao, F. Shen, Y. Zhang, J. Wang, K. Cui, H. Wang, T. Lv, T. Fu, T. Tan, Microstructure and Mechanical properties of carbide Reinforced TIC-Based Ultra-High Temperature ceramics: A review. *Coatings*, 11(12), 2021: 1444. <https://doi.org/10.3390/coatings11121444>
- [15] A. Bhat, G. Kakandikar, A. Deshpande, A. Kulkarni, D. Thakur, Characterization of Al<sub>2</sub>O<sub>3</sub> reinforced Al 6061 metal matrix composite. *Material Science Engineering and Applications*, 1(1), 2021: 11–20. <https://doi.org/10.21595/msea.2021.22028>
- [16] B.L. Dasari, M. Morshed, J.M. Nouri, D. Brabazon, S. Naher, Mechanical properties of graphene oxide reinforced aluminium matrix composites. *Composites Part B Engineering*, 145, 2018: 136–144. <https://doi.org/10.1016/j.compositesb.2018.03.022>
- [17] T.G. Aguirre, B.W. Lamm, C.L. Cramer, D.J. Mitchell, Zirconium-diboride silicon-carbide composites: A review. *Ceramics International*, 48(6), 2022: 7344–7361. <https://doi.org/10.1016/j.ceramint.2021.11.314>
- [18] C.P. Selvan, L. Girisha, V. Koti, M. Madgule, M. B. Davanageri, A. Lakshmikanthan, M.P.G. Chandrashekarappa, Optimization of stir casting and drilling process parameters of hybrid composites. *Journal of Alloys and Metallurgical Systems*, 3, 2023: 100023. <https://doi.org/10.1016/j.jalmes.2023.100023>
- [19] M.R. Shivakumar, M.K. Panchangam, Multi-response optimization of reinforcement parameters of aluminum alloy composites by Taguchi method and grey relational analysis. *Heliyon*, 10(9), 2023: e30183. <https://doi.org/10.1016/j.heliyon.2024.e30183>
- [20] P. Jayaraman, L.M. Kumar, Multi-response Optimization of Machining Parameters of Turning AA6063 T6 Aluminium Alloy using Grey Relational Analysis in Taguchi Method. *Procedia Engineering*, 97, 2014: 197–204. <https://doi.org/10.1016/j.proeng.2014.12.242>
- [21] B.N. Mordyuk, G.I. Prokopenko, Y.V. Milman, M.O. Iefimov, K.E. Grinkevych, A.V. Sameljuk, I.V. Tkachenko, Wear assessment of composite surface layers in Al–6Mg alloy reinforced with AlCuFe quasicrystalline particles: Effects of particle size, microstructure and hardness. *Wear*, 319(1–2), 2014: 84–95. <https://doi.org/10.1016/j.wear.2014.07.011>

- [22] D. Klobčar, F. Pušavec, D. Bračun, I. Garašić, Z. Kožuh, A. Venc, U. Trdan, Influence of Friction Riveting Parameters on the Dissimilar Joint Formation and Strength. *Materials*, 15(19), 2022: 6812.  
<https://doi.org/10.3390/ma15196812>
- [23] Z.S. Toor, M.M. Zafar, Corrosion degradation of aluminium alloys using a computational framework. *Tribology and Materials*, 1(4), 2022: 150–156.  
<https://doi.org/10.46793/tribomat.2022.019>
- [24] Z.C. Linn, W.W.M. Swe, A.K. Soe, A. K. Latt, Experimental and numerical analysis on the thermal performance of the aluminium absorber. *Tribology and Materials*, 2(4), 2023: 162–171.  
<https://doi.org/10.46793/tribomat.2023.020>
- [25] A. Sannino, H. Rack, Dry sliding wear of discontinuously reinforced aluminum composites: review and discussion. *Wear*, 189(1–2), 1995: 1–19.  
[https://doi.org/10.1016/0043-1648\(95\)06657-8](https://doi.org/10.1016/0043-1648(95)06657-8)
- [26] S. Gajević, L. Ivanović, A. Skulić, B. Stojanović, A review on mechanical properties of aluminium-based metal matrix nanocomposites. *Tribology and Materials*, 2(3), 2023: 114–127.  
<https://doi.org/10.46793/tribomat.2023.014>
- [27] I. Bobić, J. Ružić, B. Bobić, M. Babić, A. Venc, S. Mitrović, Microstructural characterization and artificial aging of compo-casted hybrid A356/SiC<sub>p</sub>/Gr<sub>p</sub> composites with graphite macroparticles. *Materials Science and Engineering: A*, 612, 2014:7–15.  
<https://doi.org/10.1016/j.msea.2014.06.028>
- [28] M.C. Flemings, Behavior of metal alloys in the semisolid state. *Metallurgical Transactions A*, 22(5), 1991: 957–981.  
<https://doi.org/10.1007/bf02661090>
- [29] E.d. Freitas, M. Ferrante, C.T. Ruckert, W.W.B. Filho, Thixocasting of an A356 alloy: Fluidity, porosity distribution and thermomechanical fatigue behavior. *Materials Science and Engineering: A*, 479(1–2), 2007:171–180.  
<https://doi.org/10.1016/j.msea.2007.06.037>
- [30] A. Venc, I. Bobić, Z. Mišković, Effect of thixocasting and heat treatment on the tribological properties of hypoeutectic Al–Si alloy. *Wear*, 264(7–8), 2007: 616–623.  
<https://doi.org/10.1016/j.wear.2007.05.011>
- [31] S.S.K. Reddy, C. Sreedhar, S. Suresh, Investigations on Al 7075 /nano-SiC/ B4C hybrid reinforcements using liquid casting method. *Materials Today Proceedings*, 46, 2021: 8540–8547.  
<https://doi.org/10.1016/j.matpr.2021.03.536>
- [32] A. Kareem, J.A. Qudeiri, A. Abdudeen, T. Ahammed, A. Ziout, A Review on AA 6061 Metal Matrix Composites Produced by Stir Casting. *Materials*, 14(1), 2021: 175.  
<https://doi.org/10.3390/ma14010175>
- [33] N. Tenali, G. Ganesan, P.R. Babu, An investigation on the mechanical and tribological properties of an ultrasonic-assisted stir casting Al-Cu-Mg matrix-based composite reinforced with agro waste ash particles. *Applied Engineering Letters*, 9(1), 2024: 46–63.  
<https://doi.org/10.46793/aeletters.2024.9.1.5>
- [34] P. Shantharaj, A. Prashanth, M. Nagaral, V. Bharath, V. Auradi, K. Dharshan, Microstructure, tensile and compression behaviour of B4C particles reinforced Al7075 matrix composites. *Materials Today Proceedings*, 52, 2022: 1135–1139.  
<https://doi.org/10.1016/j.matpr.2021.11.008>
- [35] J.J. Moses, I. Dinaharan, S.J. Sekhar, Characterization of Silicon Carbide Particulate Reinforced AA6061 Aluminum Alloy Composites Produced via Stir Casting. *Procedia Materials Science*, 5, 2014: 106–112.  
<https://doi.org/10.1016/j.mspro.2014.07.247>
- [36] S. Gajević, A. Marković, S. Milojević, A. Ašonja, L. Ivanović, B. Stojanović, Multi-Objective optimization of tribological characteristics for aluminum composite using Taguchi Grey and TOPSIS approaches. *Lubricants*, 12(5), 2024: 171.  
<https://doi.org/10.3390/lubricants12050171>
- [37] B. Stojanović, S. Gajević, N. Kostić, S. Miladinović, A. Venc, Optimization of parameters that affect wear of A356/Al<sub>2</sub>O<sub>3</sub> nanocomposites using RSM, ANN, GA and PSO methods. *Industrial Lubrication and Tribology*, 74(3), 2022: 350–359.  
<https://doi.org/10.1108/ilt-07-2021-0262>
- [38] S. Veličković, B. Stojanović, M. Babić, I. Bobić, Optimization of tribological properties of aluminum hybrid composites using Taguchi design. *Journal of Composite Materials*, 51(17), 2016: 2505–2515.  
<https://doi.org/10.1177/0021998316672294>
- [39] A. Venc, B. Stojanović, R. Gojković, S. Klančnik, A. Cziřra, K. Jakimovska, M. Harničárová, Enhancing of ZA-27 alloy wear characteristics by addition of small amount of SiC nanoparticles and its optimisation applying

- Taguchi method. *Tribology and Materials*, 1(3), 2022: 96–105.  
<https://doi.org/10.46793/tribomat.2022.014>
- [40] C. Parswajinan, B.V. Ramnath, M. Vetrivel, C. Elanchezhian, K. Loganathan, R. Sarvesh, C.R. Prasanna, R.K. Babu, Experimental Investigation of Mechanical and Chemical Properties of Aluminium Reinforced with MWCNT. *Applied Mechanics and Materials*, 766–767, 2015: 287–292.  
<https://doi.org/10.4028/www.scientific.net/amm.766-767.287>
- [41] B.V. Ramnath, C. Parswajinan, C. Elanchezhian, S.V. Pragadeesh, C. Kavin, P. Ramkishore, V. Sabarish, Experimental Investigation on Compression and Chemical Properties of Aluminium Nano Composite. *Applied Mechanics and Materials*, 680, 2014: 7–10.  
<https://doi.org/10.4028/www.scientific.net/amm.680.7>
- [42] S. Gudipudi, S. Nagamuthu, K.S. Subbian, S.P.R. Chilakalapalli, Enhanced mechanical properties of AA6061-B4C composites developed by a novel ultra-sonic assisted stir casting. *Engineering Science and Technology an International Journal*, 23(5), 2020: 1233–1243.  
<https://doi.org/10.1016/j.jestch.2020.01.010>